Geophys. J. R. astr. Soc. (1974), **39**, 111–121.

Earthquake Prediction: Modification of the Earth Tide Tilts and Strains by Dilatancy

Christopher Beaumont and Jon Berger

(Received 1974 May 10)*

Summary

Numerical solutions for the earth tide on a model earth with elastic dilatant crustal inclusions indicate that up to 60 per cent changes in the tilt and strain tides result from a 15 per cent reduction of V_p, the seismic p velocity, in the inclusion. The fractional changes in the tilt and strain tide amplitudes are proportional to the changes in Poisson's ratio and inverse areal bulk modulus of the inclusion and are not proportional to the V_p/V_s ratio. Further, detectable changes in the tidal amplitude will occur to a distance of 1·5 times the typical dimension of the dilatant inclusion. Monitoring the earth tide is therefore suggested as a sensitive and continuous method of earthquake prediction if such dilatancy precedes earthquakes. The time dependence of the tidal signal, due to dilatancy, will be the same as that of the V_p/V_s ratio if the dilatant material is elastic. A search of the tidal strain data from the laser strain meters at the Piñon Flat Geophysical Observatory reveals no evidence of anomalous changes in the tidal signal during the past three years. The limits of detection for changes in the tidal admittance are ± 2 per cent for a 696 hr averaging period.

Introduction

The observation of changes in the ratio of seismic velocities, V_p/V_s, prior to earthquakes (**1–5**) has provided new impetus to the problem of earthquake prediction. A current theory (**6**) is that the V_p/V_s anomaly, which is predominantly a variation in V_p, is caused by dilatancy in the earthquake source region. Dilatancy, as observed in controlled laboratory experiments, (**7**) is an inelastic volume increase that a rock undergoes near failure. The volumetric increase is caused by the creation and growth of microfractures. The dilatancy theory of earthquakes suggests that dilatancy in the Earth's crust will initially result in a strengthening (dilatancy hardening) of the rock because the effective pressure (tectonic pressure–pore pressure) is reduced. When water or steam has permeated into the dilatant volume, however, pore pressure will increase, dilatancy hardening will disappear, and any increase in tectonic pressure will then result in failure of the rock, most often in the form of an earthquake.

Scholz, Sykes & Aggarwal (**7**) list a series of precursory phenomena that might be expected to accompany dilatancy or variations in pore pressure. These include (1) distortion of the Earth's surface (as observed by vertical movements, tilt and

* Received in original form 1974 April 2.

strain), (2)V_p/V_s variations, (3) changes in electrical resistivity, (4) changes in the rate of groundwater flow, and (5) variations in the number of foreshocks as a function of time.

We report here another precursory phenomenon which provides a very sensitive way of detecting dilatancy. We conclude from the results of numerical modelling that the periodically varying tilt and strain field of the earth tide will be significantly altered by the existence of dilatancy in the crust. Modification of the elastic properties in a dilatant region will result in a variation in the tidal admittance (the normalized response of the Earth to the tidal potential). We will show that because the tidal admittance is changed more than V_p/V_s for the same change in elastic properties, the variation in admittance may provide a more sensitive indicator of dilatancy than V_p/V_s, and in so far as dilatancy precedes earthquakes, a better earthquake predictor as well.

The model

Fig. 1 illustrates the geometry of the finite element representation of the Earth used to determine the modification of the north–south component of the earth tide in the vicinity of a dilatant region. Only material within the shaded annular zone is modelled with finite elements, including the dark annulus representing the anomalous dilatant region. The choice of an axisymmetric representation allows us to apply the appropriate tidal displacements at the boundary nodes more easily than can be done with a two-dimensional model. The dimensions of the modelled zone (200 km deep by 2200 km (20°) along the surface) are chosen to make the boundaries sufficiently distant from the dilatant region that its presence does not affect the strains at the boundaries. Therefore, boundary conditions appropriate to the M_2 tide (principal lunar semi-diurnal) on a laterally homogeneous earth may be used. Distributed nodal forces are used to simulate the gravitational body force acting on each volume of mass within the model.

The model results are strictly applicable only to the M_2 tide at latitudes 20° to 40°. Additional solutions with modified boundary conditions are necessary to determine whether the results may be generalized to other latitudes and other tidal constituents.

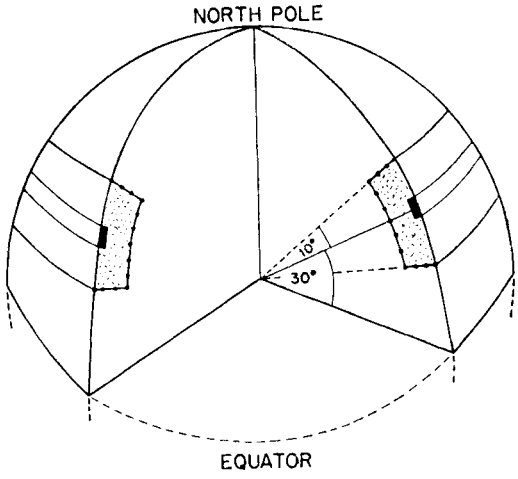

FIG. 1. Upper hemisphere of the axisymmetric finite element earth model. Lightly shaded area represents the area actually modelled with finite elements. Darkly shaded area represents the dilatant zone.

Observations reported to date (**5, 8**) indicate that, during a dilatant period, the crustal P and S velocities may be reduced as much as 20 per cent and 10 per cent, respectively. No evidence has been given for variations in mantle seismic velocities. We have used these velocity variations to model Young's modulus (E) and Poisson's ratio (σ) within a dilatant region according to the relations

$$E = \rho(3V_p^2 - 4V_s^2)/((V_p/V_s)^2 - 1)$$

$$\sigma = 0{\cdot}5\left[1 - \frac{1}{((V_p/V_s)^2 - 1)}\right]$$

keeping the density (ρ) constant. It is valid to equate the change in seismic-frequency elastic parameters with the change in the tidal-frequency elastic parameters. Any weak frequency dependence of the elastic parameters will result in an insignificant underestimate of the change in elastic properties at tidal frequencies.

The spatial extent of dilatant zones is less well known than the elastic properties. Their maximum depth is probably limited by the depth of the ' brittle zone ' estimated to be 20 km in California. This estimate is supported by the lack of mantle seismic velocity anomalies and the shallow depths of earthquakes. The modelled dilatant zones therefore have a maximum depth of 20 km. The choice of areal extent is based on the proposal that the characteristic length of a dilatant zone is linearly related to the length of the subsequent earthquake rupture zone and, consequently, to the magnitude of the earthquake (**9**). Our choice of 40 km for the length of the basic-model dilatant zone corresponds with either a magnitude 6·2 or 4·3 earthquake depending on whether the dilatant zone is two (**7**), or eight (**9**) times as large as the rupture length. The results may be linearly scaled for smaller dilatant zones, corresponding to smaller earthquakes, since the results are only weakly dependent on the layering in the model. The results may not be scaled for larger earthquakes without increasing the depth of the dilatant region. Therefore, for large earthquakes the results of calculations for a one-sided dilatant region are included.

The finite element solution provides the radial and tangential displacements of each of the surface nodal points. These displacements are differentiated numerically by cubic spline interpolation, to give the north–south components of tilt and strain. Thus, the tilt used here is just the slope of the deformed surface. The earth-tide tilt measured by a tiltmeter is related to the gravitational potential by D, the diminishing factor. $D = (1+k-h)$ where h and k are the Love numbers. Dilatancy will modify only the h part of the diminishing factor, that is, the slope of the Earth's surface. There will be no change in the direct acceleration and virtually no change in k as it is dependent on the deformation of the Earth as a whole and not on the small perturbations of the deformation caused by a dilatant region.

Modelling results

Fig. 2 illustrates the north–south components of radial displacement, surface tilt, and surface strain as a function of V_p reduction in the dilatant zone. The results are normalized by the radial displacement, tilt and strain for the corresponding non-dilatant model, also shown on the figure. The normalized plots represent the fractional change, or anomaly, in the tidal amplitudes caused by dilatancy. The surface displacement anomaly is too small to be detected with a gravimeter, but both the tilt and strain anomalies will be readily detectable, as we shall demonstrate.

That the tilt and strain anomalies are both edge effects is immediately obvious. As we proceed into a dilatant region both anomalies decrease, and become undetectable toward the centre of a very large homogeneous dilatant region. The extent of the anomalies into the dilatant region is shown in Fig. 3, which illustrates

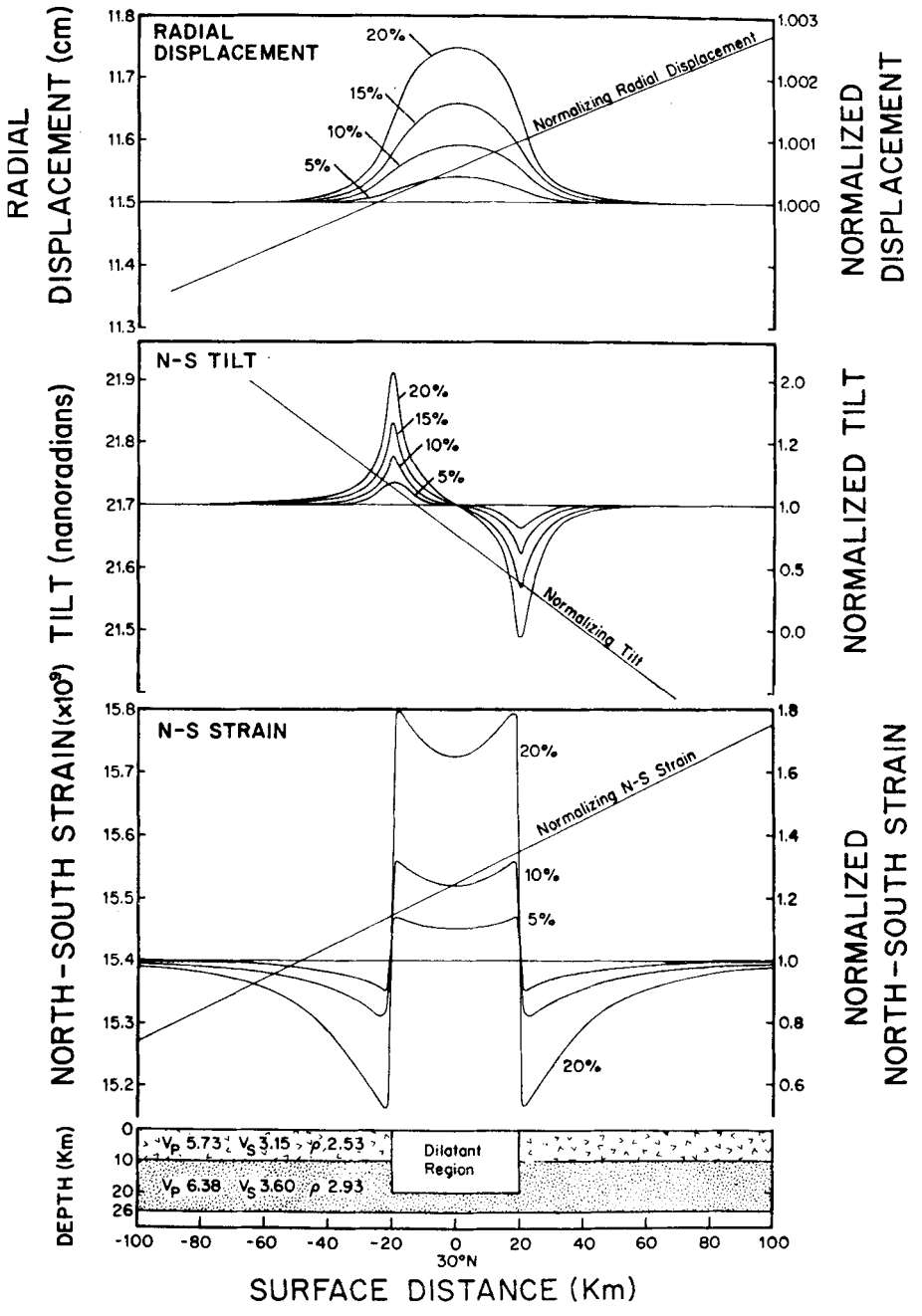

FIG. 2. North–south components of the radial displacement, tilt and strain tide amplitude for the model shown at the bottom of the figure. Model properties below 26 km follow the Gutenburg–Bullen A model. Normalizing functions are those for the same model without a dilatant inclusion. The normalized functions represent the fractional change in radial displacement, tilt and strain, as a function of position, when the *P*-velocity in the dilatant region is reduced by 5, 10, 15 and 20 per cent.

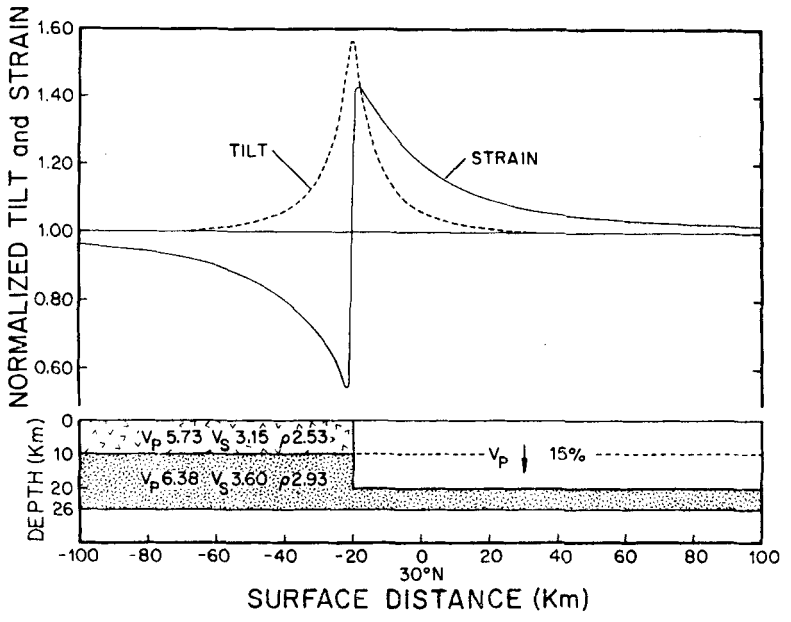

FIG. 3. North–south components of the normalized tilt and strain tide amplitude across the edge of an infinitely wide dilatant zone. Model properties below 26 km are based on the Gutenburg–Bullen A model. The normalizing model has no dilatant region.

the effect across the edge of an infinitely wide dilatant region. The strain results are particularly encouraging, suggesting that a 15 per cent decrease in V_p produces a 2 per cent tidal strain anomaly even at a distance of 120 km from the edge of the dilatant region. The narrower tilt anomaly is greater than 2 per cent at distances less than 30 km from the boundary.

Fig. 4 illustrates the calculation results for other geometrics including: (1) dilatant regions that do not extend to the surface, (2) an ellipsoidal dilatant region, and (3) a model where there is a gradation in dilatancy from the external non-dilatant zone to a central dilatant core. For all models the characteristic anomaly shape persists. The effects of smoothing the geometry, burial, or grading the dilatant region are similar, and result in the removal of the high frequency content of the anomaly. Both the tilt and strain anomalies remain significant, however, several tens of kilometres from the boundaries.

The numerical results may be parameterized in order to relate the changes in elastic properties, due to arbitrary V_p and V_s changes, to the surface displacement, tilt, and strain anomalies calculated by the finite element models. The results of this parametrization are illustrated by Figs 5 and 6 which plot the anomaly maximum versus both V_p reduction (holding V_s constant) and a characteristic elastic parameter that determines the anomaly maximum for arbitrary changes in both V_p and V_s. The dashed and solid lines are determined by keeping V_s constant and varying V_p. The asterisks plot some additional results corresponding to the changes in both V_p and V_s that are indicated on the figures. The amount by which the asterisks depart from the nearest line is an estimate of the failure of the parameter to account totally for the anomaly maximum when V_p and V_s are both varied. Because these departures are small, and the lines nearly straight, we conclude that the anomaly maxima are approximately functions of one variable, the Poisson's ratio contrast, for tilt and

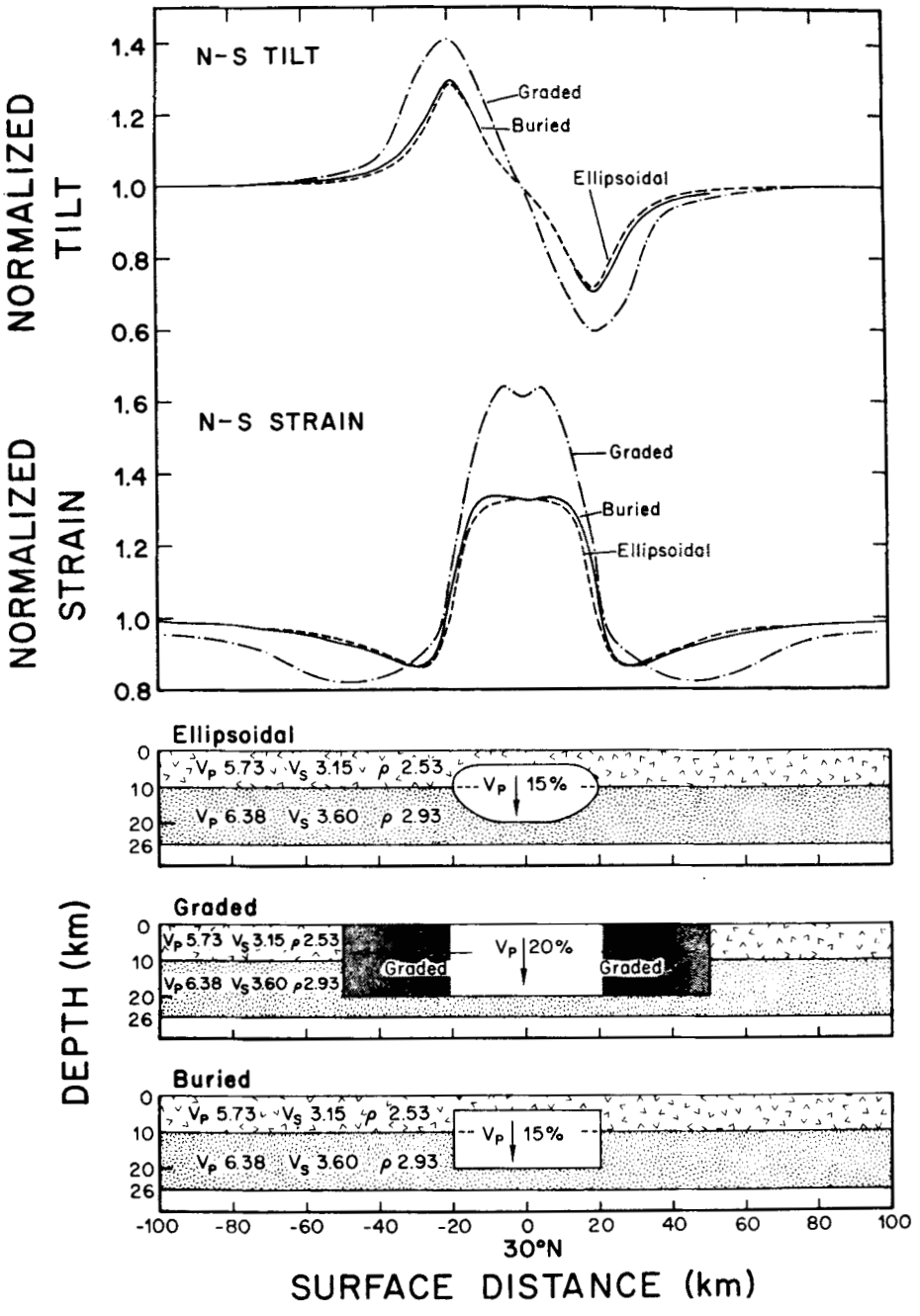

FIG. 4. North–south components of the normalized tilt and strain tide amplitude for ellipsoidal, graded and buried dilatant zones. Model properties below 26 km are based on the Gutenburg–Bullen A model. The depth to the upper boundary of the ellipsoidal and buried zones is 4 km. In the graded model, V_p is reduced by 20 per cent in the central region. V_p linearly decreases outwards to the boundary with the non-dilatant zone.

elevation, and the $(\lambda+\mu)^{-1}$ contrast for tangential displacement and strain. Contrast means the ratio of the values of the parameter inside and outside the dilatant region, at the same depth. $(\lambda+\mu)$ is the areal strain equivalent of the bulk modulus $(\lambda+2/3\mu)$, and is termed the 'areal bulk modulus'.

The graphs therefore generalize the results of Fig. 2 to arbitrary changes in V_p and V_s and to a range of depths of the dilatant region. If the changes in V_p and V_s are known, they can be used to calculate the Poisson's ratio contrast, and the areal bulk modulus contrast. The graphs can then be used to estimate the anomaly maxima for various possible depths of the dilatant region. Although the graphs are explicitly plotted for a 40 km dilatant region, it should be remembered that they approximately scale to smaller dilatant regions having the same shape.

The graphs illustrate that the anomaly size is a function of both V_p and V_s and not a function of V_p/V_s. For example, from Fig. 6, we see that a decrease in both V_p

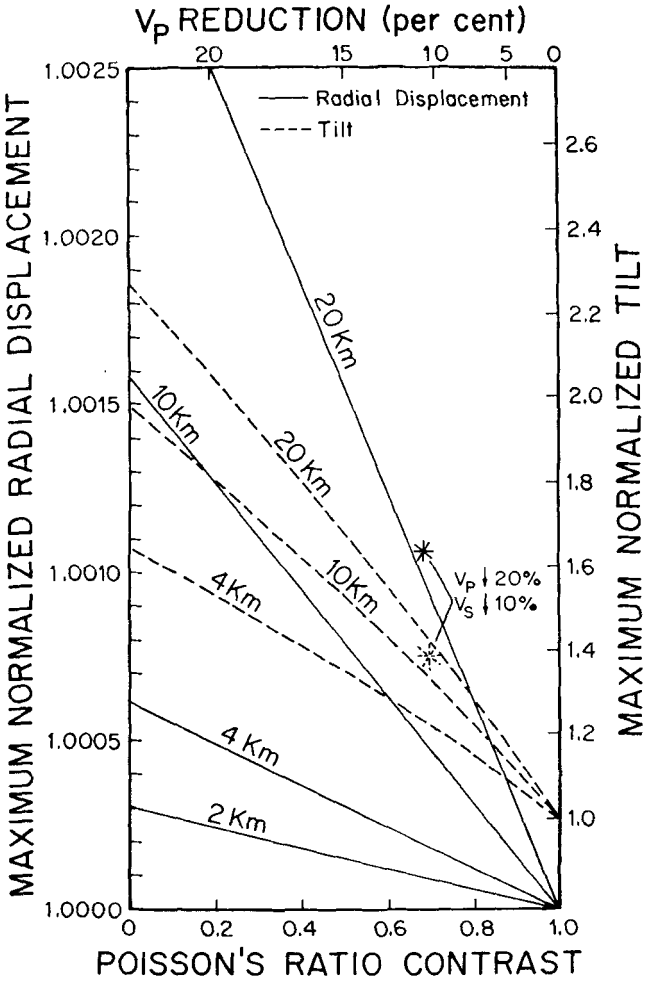

FIG. 5. Plot of the maxima of normalized radial displacement and normalized tilt versus V_p reduction in the dilatant zone (V_s and ρ constant) and the Poisson's ratio contrast. The results are for a rectangular dilatant zone, as shown in Fig. 2, but a range of dilatant zone depths are included. The asterisks plot theoretical results for a 20 km × 40 km zone in which V_p and V_s are reduced by 20 per cent and 10 per cent, respectively.

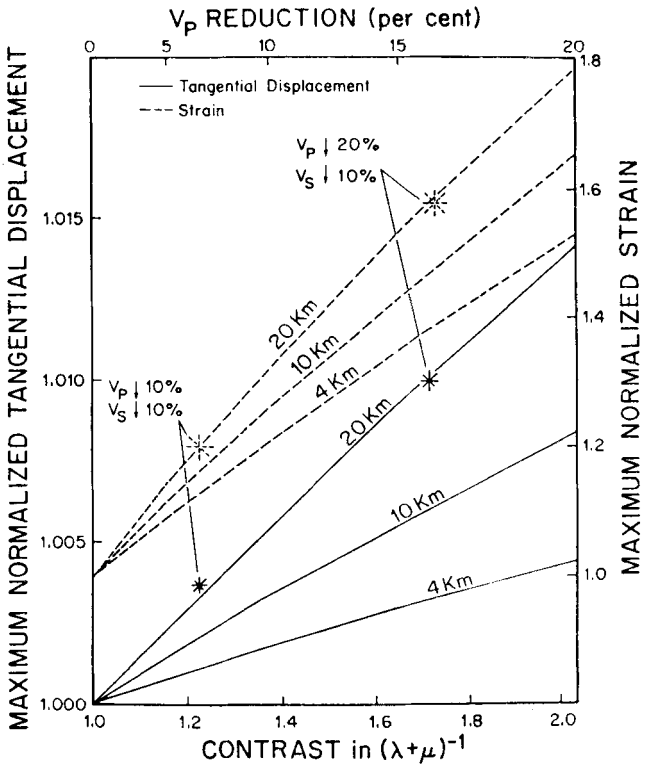

FIG. 6. Plot of the maxima of normalized tangential displacement and normalized strain versus V_p reduction in the dilatant zone (V_s and ρ constant) and the contrast in inverse ' areal bulk modulus '. The results are for a rectangular dilatant zone, as shown in Fig. 2, but a range of dilatant zone depths are included. The asterisks plot theoretical results for 20 km × 40 km zones in which V_p and V_s are respectively reduced by 20 per cent and 10 per cent, and 10 per cent and 10 per cent.

and V_s by 10 per cent which will result in only a small V_p/V_s anomaly, produces a 20 per cent change in strain when the depth of the dilatant zone is 20 km. Fig. 8 also demonstrates that the strain anomaly is not strongly dependent on the depth of the dilatant region, a result indicating that even shallow dilatant zones should be detectable as a temporal variation in the tidal strain admittance.

Observational results

On the basis of these calculations, we have examined the strain data from the three component laser strainmeter at the Pinon Flat Observatory (**10**) (located at 32° N) in an attempt either to discover significant changes in the tidal admittance that would be caused by a nearby dilatant region, or to set practical limits on the detectability of changes in the M_2 admittance.

The tidal admittance observed by a strainmeter located outside a dilatant region, but close enough to detect its effects, is expected to exhibit a temporal character similar to that of V_p/V_s. That is, initially the admittance would decrease rapidly as dilatancy begins and then return slowly to normal. Conversely, if the strainmeter were located above a dilatant region, the admittance would initially increase signalling the onset of dilatancy and subsequently return slowly to its normal value.

Each strain record was divided into contiguous 696-hr segments, a length that reduces the side-band contamination of the main solar tidal constituents. The theoretical strain tide on an oceanless laterally homogeneous earth was calculated for the three directions and similarly divided. Fourier analyses of the theoretical and observed strains for each component were then examined for changes in the magnitude of the ratio of the observed to theoretical M_2 Fourier amplitudes as a function of time. The results are shown in Fig. 7.

Due to the presence of earth noise in the strain record, the limits of detectability will be set by the noise power in the resolved M_2 bandwidth. As this bandwidth is inversely related to the record length, the limits of detectability will improve as the section length increases. At two cycles per day, the Earth's strain noise is approximately $2\times10^{-14}\,(\Delta l/l)^2$/Hz (**11**). Thus, for a record T hr in length the rms noise in the M_2 band will be

$$\frac{2{\cdot}4\times10^{-9}}{\sqrt{T}}\left(\frac{\Delta l}{l}\right)$$

and for a record of 696 hr, the noise will contribute $9\times10^{-11}\,(\Delta l/l)$ rms to the estimate of its M_2 amplitude. The 95 per cent confidence limits dictated by the noise level estimates are indicated in Fig. 7. The limits of detectability for the east component are approximately twice those for the other two components simply because the M_2 tide is smaller by that factor in the east–west direction while the noise is approximately the same. A further reduction in the detectability limits may be achieved by correlating the behaviour of the admittance of other tidal constituents with that of M_2.

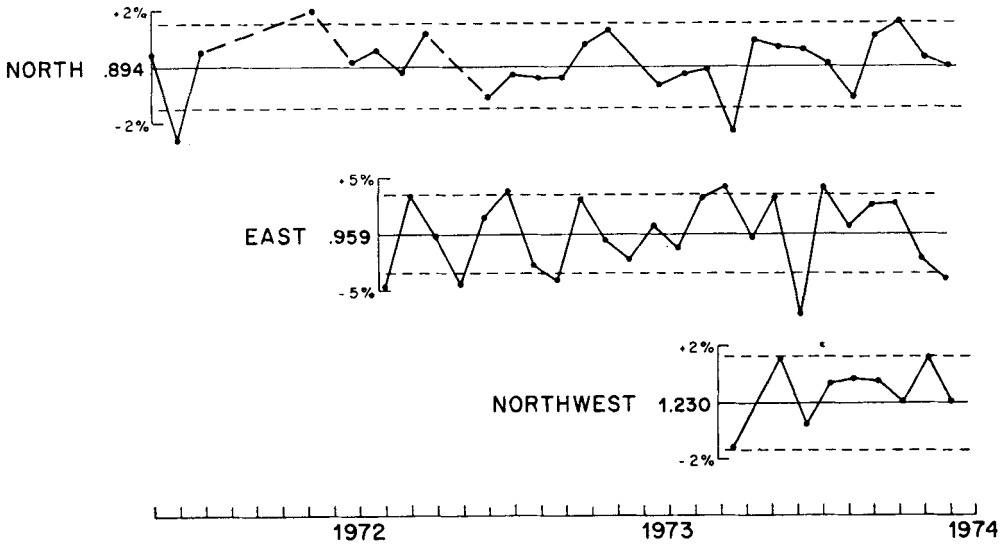

FIG. 7. Variation in north, east and north-west components of the M_2 tidal strain admittance at the Piñon Flat Observatory for the period 1971 to 1974. Each point represents the ratio of the M_2 Fourier amplitude estimate, from an independent 696-hr section of the observed record, to a similar estimate of the theoretical M_2 tide. The means of the estimates, 0·894, 0·959, 1·230 are not equal to unity because the M_2 ocean tide load modifies the observed strain tide at Piñon. The 95 per cent confidence limits are average confidence limits and may vary by a factor of 2 from noisy to quiet intervals.

Conclusions

The model results indicate that large variations (50 per cent) in the earth tide tilt and strain accompany even moderate (15 per cent) V_p/V_s changes. The examination of strain data from the Pinon Flat Observatory leads us to the following conclusions. (1) The M_2 tidal admittance has not changed significantly during the last 3 years; hence, there is no evidence for dilatancy changes near Pinon Flat. Neither would nearby seismicity have dictated dilatancy detectable at the observatory. (2) The practical limits of dilatancy detection by this method are set by the ambient earth noise at the tidal constituent period. For a one-month interval tidal admittance changes as small as ± 2 per cent can be detected at the 95 per cent confidence level, for a 1×10^{-8} amplitude M_2 strain tide. This result implies that, for example, a dilatant region 20 km $\times$ 40 km in which V_p is reduced by 15 per cent could be detected by a strainmeter located up to 100 km from its centre. Similarly, for an earth tilt noise of approximately 3×10^{-12} radians^2/Hz (**12**) at the M_2 frequency, the limits of detectability for variations in tilt admittance are ± 5 per cent for a tilt tide amplitude of 5×10^{-8} radians. Hence, when it is taken into account that only one half of the tilt tide is due to the slope of the Earth's surface, the dilatant region used in the above example could be detected by a tiltmeter located up to 35 km from its centre.

In summary, if V_p/V_s anomalies are indeed earthquake precursors accurate observations of earth tide tilt and strain will provide sensitive earthquake predictors. Further, these techniques have some potential advantages over the direct seismic observation of V_p/V_s. First, the technique is aseismic; no background earthquake activity or refraction profiling is necessary in order to sample the nearby elastic properties. The tidal technique should therefore find immediate application in relatively aseismic areas. Second, the earth tide provides a spatially deterministic input signal, so there are no problems analogous to those of locating earthquake hypocentres and identifying particular ray paths. Third, the earth tide provides a temporally continuous input signal so that elastic properties can be sampled continuously. The capability of this method to detect changes in the elastic properties is inversely related to the square root of the averaging period. For example, the precursor time for a moderate earthquake (magnitude = 6) is estimated to be 500 days (**7**), sufficient time for 17 independent 30 day estimates of the tidal admittance. With a one day average, strain admittance changes greater than ± 10 per cent are detectable. Consequently, dilatancy associated with earthquakes as small as magnitude 2 is detectable. Finally, the tidal strain and tilt represent a spatially integrated sample of the elastic properties and can be used to distinguish between bulk elastic changes and changes in anisotropy.

Acknowledgments

This work was jointly supported by the La Jolla Foundation for Earth Sciences, National Science Foundation Grant No. Ga 40948X, United States Geological Survey Grant No. USDI GS-14-08-0001-G-73 and National Aeronautical and Space Administration Grant No. NGR 05-009-246. The authors wish to thank W. E. Farrell and R. L. Parker for critically reading the manuscript.

Institute of Geophysics and Planetary Physics,
University of California, San Diego.

References

(1) Savarenky, E. F., 1968. *Tectonophysics*, **6**, 17.
(2) Semenov, A. N., 1969. *Izv. Acad. Sci. USSR Phys. Solid Earth*, **4**, 245.

(3) Nersesov, I. L., Semenov, A. N. & Simbireva, I. G., 1969. In *The physical basis of foreshocks*, Nauka, Moscow.
(4) Aggarwal, Y. P., Syker, L. R., Armbruster, J. & Sbar, M. L., 1973. *Nature*, **241,** 101.
(5) Whitcomb, J. H., Garmany, J. D. & Anderson, D. L., 1973. *Science*, **180,** 632.
(6) Nur, A., 1972. *Bull. seism. Soc. Am.*, **62,** 1217.
(7) Scholz, C. H., Sykes, L. R. & Aggarwal, Y. P., 1973. *Science*, **181,** 803.
(8) Richards, P. G. & Aggarwal, Y. P., 1973. *EOS Trans. Am. geophys. Un.*, **54,** 1134.
(9) Anderson, D. L. & Whitcomb, J. H., 1973. In Proceedings of the Conference on Tectonic Problems of The San Andreas Fault System, *Stanford University Publications in the Geological Sciences*, **13,** 417.
(10) Berger, J. & Wyatt, F., 1973. *Phil. Trans. R. Soc. Lond. A.*, **274,** 267.
(11) Berger, J. & Levine, J. L., 1974. *J. geophys. Res.*, **79,** 1210.
(12) Lambert, A., 1969. Unpublished Ph.D. Thesis. Dalhousie University, Halifax, Canada.

Note added in proof

Dr L. A. Latynina (Institute of the Physics of the Earth, Academy of Sciences of the USSR), reported at the International Symposium on Earthquake Forerunners Searching, Tashkent, USSR, May 1974, observations of variations in the strain tide prior to an earthquake in southern Tien Shan of magnitude 5 at a distance of 20 km.